BULLETIN OF THE INTERNATIONAL INSTITUTE
OF SEISMOLOGY
AND EARTHQUAKE ENGINEERING
Vol. 6 (1969), pp. 103-142

*Contribution to Aseismic Design of Shear Structures**

By Yutaka MATSUSHIMA[1] and Panayotis G. CARYDIS[2]

Summary

The present paper is dealing with shear type structures, based almost upon an experiment held by B. R. I./Ministry of Construction on March 1969. The purpose of this experiment was to rationalize the structural and dynamic design of buildings.

A structure, in general, may be of several types as:

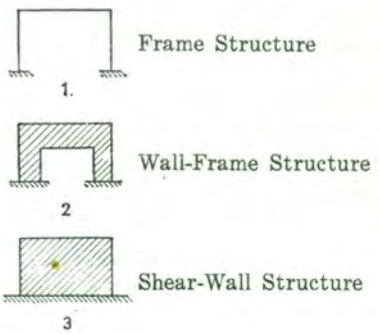

and a combination of these types.

The dynamic behaviour of a structure, besides its exciting dynamic load, depends upon the column to beam rigidity ratio, as well as upon the height to length ratio of the structure. The most common are the shear type, the bending type and a combination of these two behaviours. Considering plastic deformations of some members of the structure, the behaviour of the whole of it may be altered.

The tested structure is a 5-storey full scale apartment house consisting of reinforced concrete wall frames. This structure is considered to be of the shear type.

The special feature of this specimen lies, briefly, in its economic design which is considered to be close to the structural and working

* Manuscript received for publication on 30, October, 1969.

1) International Institute of Seismology and Earthquake Engineering.

2) On leave from the National Technical University, Athens, Greece, as a participant to the Advanced Course of IISEE in the Academic Course of 1968-1969.

m_i: Concentrated mass at floor level $i(tm^{-1}\,sec^2)$
$[M]$: The diagonal mass matrix of the structure
N_i, T_i, ω_i: Frequency, period and angular frequency of the i^{th} mode of the structure respectively (c/s, sec, sec^{-1})
N_0, T_0, ω_0: Frequency, period and angular frequency of the ground vibration respectively (c/s, sec, sec^{-1})
Q_i: Shear force at floor level $i(t)$
S_n: Spectral density ($m\,sec^{-1}$)
t_d: Duration of the ground vibration (sec)
$v_i(t)$: Relative translation of the structure at the i^{th} level with respect to the rigid base (m)
$V_i(t)$: Absolute translation of the structure at the i^{th} level (m)
$\ddot{y}(t)$: Ground acceleration (gal) or ($m\,sec^{-2}$)

Part I. The Test and its Results

1. *Explanation of the experiment.*

1a. *Test specimen.*

The plan and elevation of the test specimen as well as the whole set up of the various apparatus necessary for it are shown in Fig. 1.1 through 1.4. Main properties of the building under experiment are as follows:

1. The building consists of five storeys each of which has two apartments.
2. The area of each storey is $13(m)\times7(m)=91(m^2)$ approximately.
3. The whole structure is of about 14(m) height above the floor

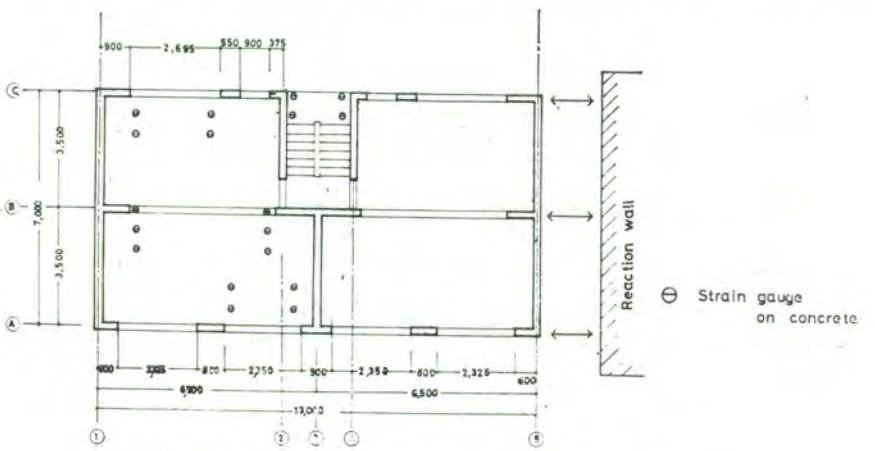

Fig. 1.1. Plan and positions of apparatus (2nd floor)

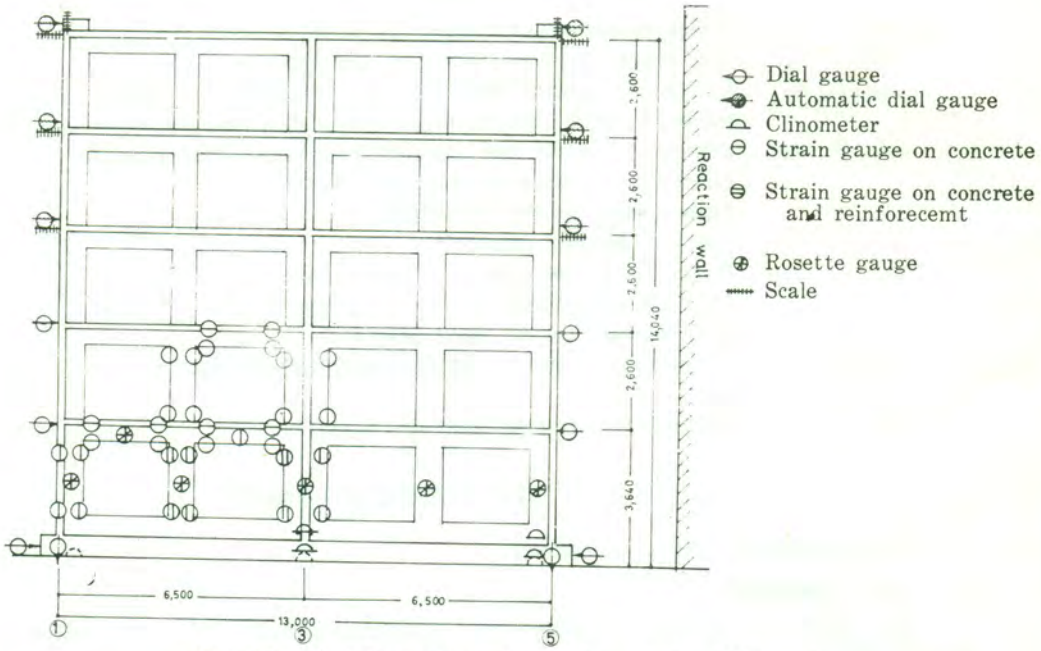

Fig. 1.2. Elevation and positions of apparatus (A-frame)

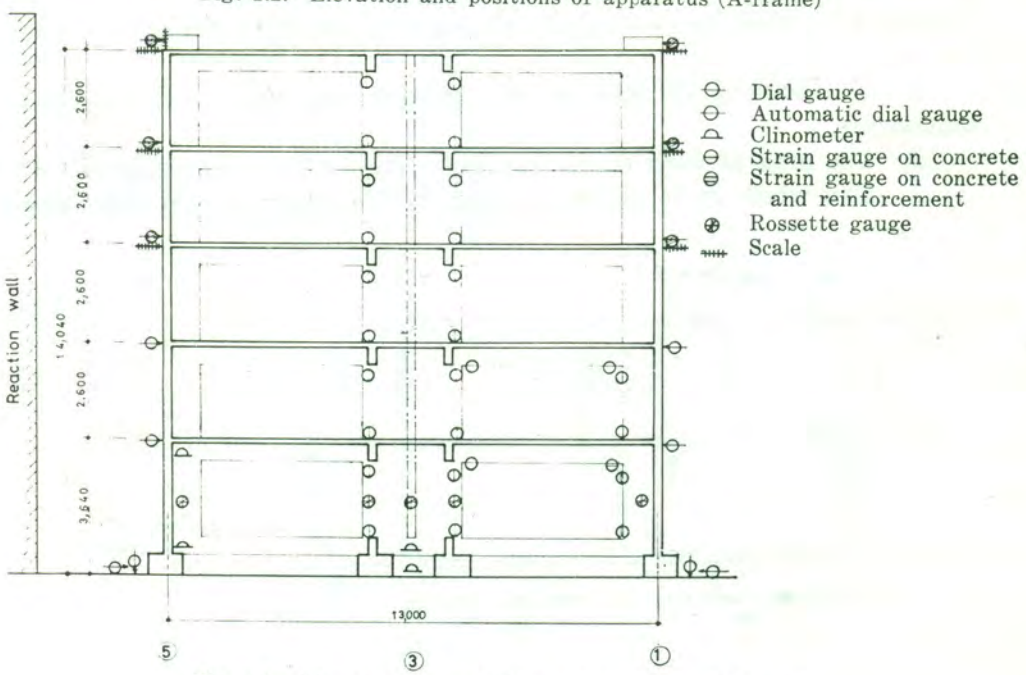

Fig. 1.3. Elevation and positions of apparatus (B-frame)

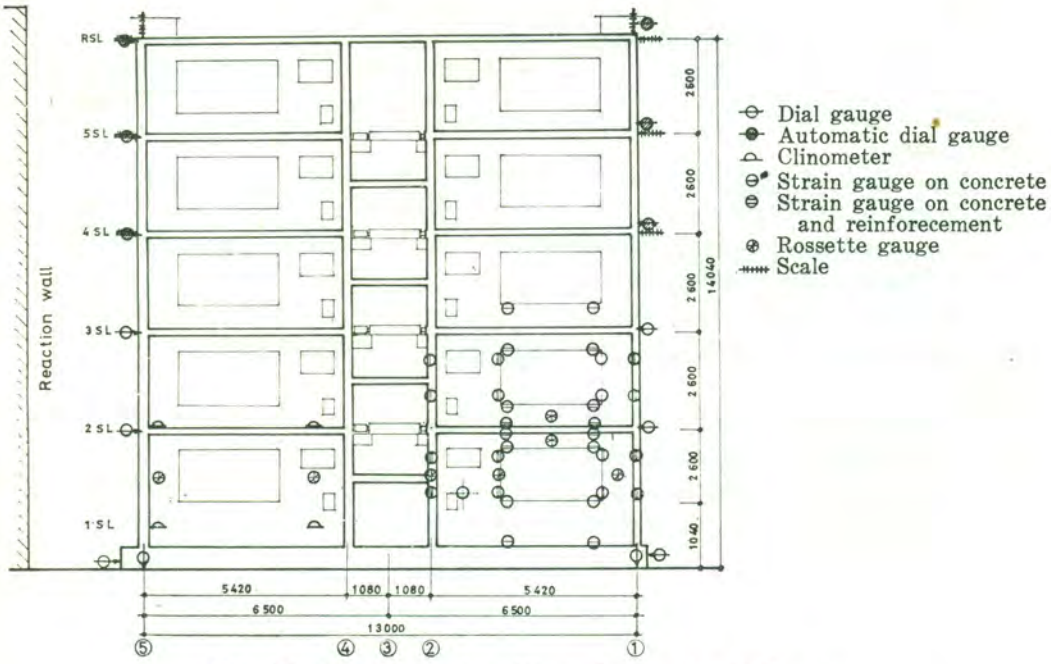

Fig. 1.4. Elevation and positions of apparatus (C-frame)

level of the testing laboratory.

4a. The total dead weight is almost 420 (ton), 320 (ton) without foundation, i.e. 64 (ton)/storey.

4b. The total dead plus live load of the real structure is almost 1.5 times the one listed on item 4a.

5. The walls in both directions are of 15(cm) thickness. The length of the wall per unit area is 12.0(cm/m^2) in the longitudinal direction, and 25.4(cm/m^2) in the transverse one.

6. The horizontal design shearing force is 89.2(ton)$\simeq$90(ton) on the first storey, which corresponds to the load scale 1.

7. The shearing stress in the wall column of the first storey in the case of design load is near to 4.9(kg/cm^2).

1b. Method of loading.

Horizontal static loading.

The reaction mechanism in the large size structures testing laboratory of Japan Housing Corporation properly equiped with twenty link oil pressure jacks (maximum load=1000(ton)) was utilized for the horizontal static loading.

The loading was performed by the following two methods:

a) Individual loading on each floor.

The static loads were acting on each floor by three uniformly pressed link jacks as shown in Fig. 1.5. Every floor was being loaded individually.

This kind of loading was being carried out at both the initial and final stage of the experiment. The main purpose of the loading under consideration was to obtain the flexibility matrices of the structure.

b) Uniformly distributed loading.

The static loads were acting on every floor by three uniformly pressed link jacks. All floors were being loaded simultaneously, as shown in Fig. 1.6.

An earthquake motion of maximum acceleration max $\ddot{y}(t)=200$ gal statically applied on the structure produces inertia forces $W=M\cdot\max\ddot{y}(t)$ $=(1.5m_i)\cdot\max\ddot{y}(t)=18$(ton)/storey, the load scale 1 is thus introduced which means that the force is 6 ton per jack. By the load scale 1 the inertia

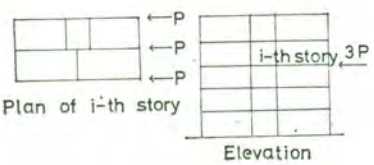

Fig. 1.5. Individual loading on each floor.

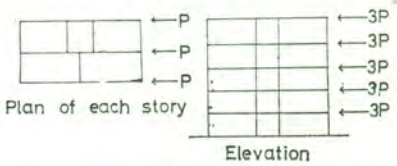

Fig. 1.6. Uniformly distributed Loading.

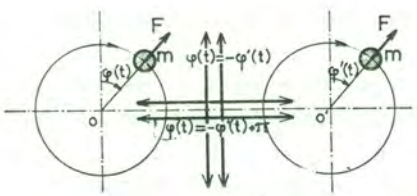

Rotating masses: $m(tm^{-1}\,\mathrm{sec}^2)$

Centr force: $F=mr\omega^2=\dfrac{M}{1000g}\omega^2$

$=\dfrac{M}{1000g}(2\pi N)^2$, (ton)

Moment: $M=1000\,\mathrm{mgr}$ (Kgm)

Frequency: $N=\dfrac{\omega}{2\pi}$ (c/s)

Accel. of gravity: $g=9.81\,\mathrm{msec}^{-2}$

Fig. 1.7. Principle of the Dynamic Exciter

forces caused by the above assumed earthquake motion acting statically on the structure is simulated. This type of loading, of course, does not correspond so much to the reality as to the design loads, besides offering simplicity.

Dynamic loading

Dynamic loads were produced by the dynamic exciter of Building Research Institute. This exciter was located on the center of the roof of the specimen, whose maximum capacity was $F=10$(ton), Fig. (1.7.). The tests were being carried out five times

Table 1.1. Day's program & contents of tests.

Date	Test (Symbol)	Content (Load scale)
3/Mar./'69 4 5	1st dynamic test (D_1)	Elastic vibration
11	1st static test (S_1)	Individual loading (+1)
12	2nd dynamic test (D_2)	Elastic vibration
14	2nd static test (S_2)	Uniformly distributed loading ($\pm$1)
18	3rd static test (S_3)	Uniformly distributed loading ($\pm$3)
19	3rd dynamic test (D_3)	Plastic vibration
20	4th static test (S_{4-1})	Uniformly distributed loading (+maximum)
24	5th static test (S_{4-2})	Uniformly distributed loading (−maximum)
26	6th static test (S_5)	Uniformly distributed loading ($\pm$maximum)
27	4th dynamic test (D_4)	Vibration after failure
28	7th static test (S_6)	Individual loading (+1)
29	5th dynamic test (D_5)	Vibration after failure

according to the progress of failure of the specimen.

1c. Measurement

The objects of the measurement are as follows. (Ref. Fig. 1.1-1.4).

1) Static measurement
   - i) Measurement of strains in concrete and reinforcements by wire strain gauges.
   - ii) Measurement of slope angles by clinometers.
   - iii) Measurement of displacements by dial-gauges and scales.
   - iv) Observation of cracks and taking photographs.

2) Dynamic measurement
   Measurement of displacements of each floor.

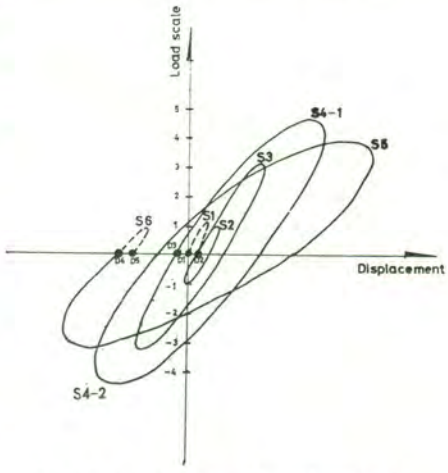

Fig. 1.8. Outline of various tests.

1d. Day's program

The experiments were being carried out on March 1969, and continued for about a month.

The day's program and contents of the tests are listed on Table 1.1. Fig. 1.8. shows them intelligibly.

1e. Properties of materials

Properties of the reinforcement and concrete obtained by the tests of materials are as follows.

Young's modulus of the reinforcement

$$E_s = 2.09 \times 10^6 \text{ kg/cm}^2 ,$$

Yielding point of the reinforcement

$$\sigma_{sy} = 3.29 \text{ } t/\text{cm}^2 ,$$

Initial Young's modulus of concrete

$$E_{ci} = 2.72 \times 10^5 \text{ kg/cm}^2 ,$$

General Young's modulus of concrete

$$E_c = 2.19 \times 10^5 \text{ kg/cm}^2 ,$$

Strength of concrete

$$F_c = 230 \text{ kg/cm}^2 .$$

2. Experimental Results

2a. The results obtained from the static tests.

1) The maximum strength for the first positive loading was 4.3 in load scale, 3.9 for the first negative one, 3.2 for the second positive one, and 2.9 for the second negative one. The ultimate strength decreased for every repetition of loading.

2) The order of the remarkable shearing cracks that occurred in the walled columns of the first storey were as follows.

i) in the short columns of *C*-frame at the stage 2.3 in load scale. ii) in the side colums of *C*-frame at about 2.7. iii) in the center columns of *B*-frame at about 3.0. iv) in the side columns of *B*-frame and all columns of *A*-frame at the maximum load scale 4.3, respectively.

3) The mean shearing stress in columns at the stage when remarkable shearing cracks occurred in the short columns of *C*-frame at load scale 2.3 becomes about 11 kg/cm^2. This value corresponds to about $0.048 F_c$.

4) The mean shearing stress in columns at the maximum load scale 4.3 becomes about 21 kg/cm², which almost corresponds to $0.091\,F_c$.

5) The relative horizontal displacement of the first storey at the maximum loading was about 1.8 cm. This corresponds to about 1/140 in the rotation angle of the storey.

6) The horizontal displacement of the top of the structure relative to the footing at the maximum loading was about 4.9 cm, which corresponds to about 0.98 cm in the mean storey displacement.

7) The stiffness of C-frame is the greatest, and that of *A*-frame the smallest. The displacements of *B*-frame and *C*-frame as compared with that of *A*-frame were about 90% and 80% respectively. These ratio were almost constant regardless of the magnitude of loading.

8) The horizontal displacements over the height were distributed in so called "shear-type" i.e., the storey displacements of the lower stories were larger than the upper. The plastic deformation of the first storey increased particularly when the load became greater, and the ratio between the deformation of the first storey to the total one reached about 40%.

2b. Results from the dynamic tests.

The fundamental natural periods and damping ratios obtained from the five various dynamic tests are tabulated in Table 2.1., whose *M* listed on the right hand side column represents the eccentricity moment of the generator.

Table 2.1. Fundamental natural periods & damping ratios

Symbols of dynamic test	Fundamental Natural period T_1 (sec)	Fundamental damping ratio (%)	Eccentricity moment *M*(kgm)
D_1	0.149	2.24	2
D_2	0.152	2.59	2
D_3	0.170	2.22	2
D_4	0.290	—	2
D_5	0.435	3.26	20
	0.465	4.65	40
	0.480	3.40	60

The structure is considered to be almost elastic in D_1 and D_2 tests, to develop into the plastic zones near to failure in D_3 test, and to be in the condition after the destruction in D_4 and D_5. The fundamental natural period increases about twice during D_1 through D_5. Moreover,

when the eccentricity moment is taken to be greater in D_5, the natural period increases three times compared with the elastic vibration. Damping ratios are a little more than 2% in cases of the small amplitude.

3. Evaluation of the data received after Static Tests & Dynamic Tests.

This section comprises two parts. In the first part an evaluation of some dynamic properties of the structure under consideration was tried based on the results of static tests, and compared them with that from the dynamic tests. The second part deals with the reverse problem, i.e. the establishment of the flexibility matrix of the structure evaluating the results of dynamic tests.

3a. Static tests

3a1. Static test S_1

At this stage the behaviour of the whole structure was perfectly elastic. (Fig. 1.8)

The absolute deformations of the storeys received there-of can be presented in the following matrix form:

$$[F'']=10^{-6}\begin{Bmatrix} 4.861 & 6.158 & 5.764 & 5.369 & 5.300 \\ 6.158 & 12.039 & 11.758 & 11.202 & 12.197 \\ 5.764 & 11.758 & 14.817 & 17.916 & 19.861 \\ 5.369 & 11.202 & 17.916 & 23.428 & 28.705 \\ 5.300 & 12.197 & 19.861 & 28.705 & 39.444 \end{Bmatrix} (mt^{-1})$$

The arithmetic statement of the diagonal mass matrix has the form as given below.

$$[M]=\begin{Bmatrix} 6.59 & — & — & — & — \\ — & 6.59 & — & — & — \\ — & — & 6.59 & — & — \\ — & — & — & 6.59 & — \\ — & — & — & — & 4.67 \end{Bmatrix} (tm^{-1}\,\mathrm{sec}^2)$$

Following the well known procedure of Stodola, after the third iteration the mode shape $\{\delta''\}_1$ is assumed to be as:

$$\{\delta''\}_1=\begin{Bmatrix} 0.222 \\ 0.454 \\ 0.633 \\ 0.808 \\ 1.000 \end{Bmatrix} \qquad (3.1a)$$

and

$$\omega_1'' = 46.435\,(\text{sec}^{-1}) \text{ or } N_1'' = 7.4\,(\text{c/s}) \text{ or } T_1'' = 0.135\,(\text{sec}) \qquad (3.1b)$$

As stated in section 2-8 (page 111), the behaviour of the building frame walls appeared close enough to the shear building hypothesis.

According to this hypothesis the above calculated coefficients f_{ij}'' lead to new values f_{ij} from [1]:

$$f_{ij} = \frac{1}{5-(i-1)} \sum_{k=i}^{5} f_{ij}'' \text{ , for } j \geq 1 \text{ .} \qquad (3.2)$$

The resulting matrix $[F]^{S_1}$ according to the shear building hypothesis is of the form:

$$[F]^{S_1} = 10^{-6} \begin{bmatrix} 5.490 & 5.490 & 5.490 & 5.490 & 5.490 \\ 5.490 & 11.799 & 11.799 & 11.799 & 11.799 \\ 5.490 & 11.799 & 17.531 & 17.531 & 17.531 \\ 5.490 & 11.799 & 17.531 & 26.066 & 26.066 \\ 5.490 & 11.799 & 17.531 & 26.066 & 39.444 \end{bmatrix} (mt^{-1})$$

A graphical comparison between these two groups of coefficients is given in Fig. 3.1.

Following the above mentioned iterative procedure the mode shape $\{\delta\}_1^{S_1}$ is finally determined as,

$$\{\delta\}_1^{S_1} = \begin{bmatrix} 0.235 \\ 0.484 \\ 0.670 \\ 0.863 \\ 1.000 \end{bmatrix} \qquad (3.3a)$$

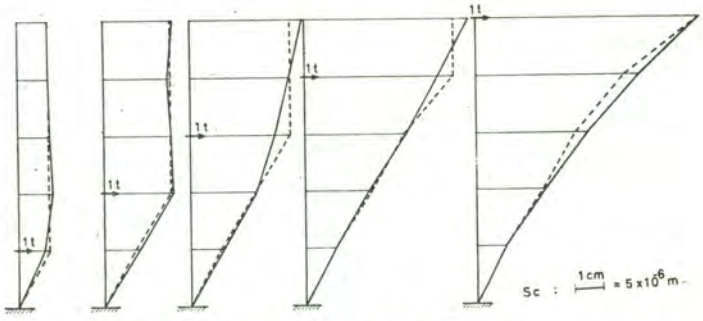

—— Flexibility coefficients after S_1.
..... Flex. coef. after simplified shear bldg. hypothesis

Fig. 3.1. Flexibility coefficients after static test S_1

and

$$\omega_1^{S_1}=46.95\,(\text{sec}^{-1}) \text{ or } N_1^{S_1}=7.47\,(\text{c/s}) \text{ or } T_1^{S_1}=0.134\,(\text{sec}) \qquad (3.3b)$$

The determined mode shape and the corresponding fundamental frequency after D_1 are as follows:

$$\{\delta\}_1^{D_1}=\begin{Bmatrix}0.260\\0.540\\0.740\\0.892\\1.000\end{Bmatrix} \qquad (3.4a)$$

and

$$\omega_1^{D_1}=41.595\,(\text{sec}^{-1}) \text{ or } N_1^{D_1}=6.62\,(\text{c/s}) \text{ or } T_1^{D_1}=0.151\,(\text{sec}) \qquad (3.4b)$$

3a2. Static Test S_5

At this stage a positive uniform loading of $3(+19.4)=58.2\,t$/storey and a negative one of $3(-17.2)=-51.6\,t$/storey was applied. Due to some technical misarrangement during the negative loading the deformations were not so reliable and only the results after the positive loading were taken into consideration.

The flexibility matrix so evaluated is as:

$$[F]^{S_5}=10^{-6}\begin{Bmatrix}200.00 & 200.00 & 200.00 & 200.00 & 200.00\\ 200.00 & 252.75 & 252.75 & 252.75 & 252.75\\ 200.00 & 252.75 & 300.75 & 300.75 & 300.75\\ 200.00 & 25.275 & 300.75 & 373.25 & 373.25\\ 200.00 & 252.75 & 300.75 & 373.25 & 517.25\end{Bmatrix}(mt^{-1})$$

from which is defined:

$$\{\delta\}_1^{S_5}=\begin{Bmatrix}0.599\\0.732\\0.826\\0.919\\1.000\end{Bmatrix} \qquad (3.5a)$$

and also the

$$\omega_1^{S_5}=10.949\,(\text{sec}^{-1}) \text{ or } N_1^{S_5}=1.7\,(\text{c/s}) \text{ or } T_1^{S_5}=0.573\,(\text{sec}) \qquad (3.5b)$$

The test D_5 gave respectively:

$$\{\delta\}_1^{D_5} = \begin{Bmatrix} 0.620 \\ 0.770 \\ 0.820 \\ 0.910 \\ 1.000 \end{Bmatrix} \tag{3.6a}$$

and:

$$\omega_1^{p_5} = 14.388\ (\text{sec}^{-1}) \text{ or } N_1^{p_5} = 2.29\ (\text{c/s}) \text{ or } T_1^{p_5} = 0.437\ (\text{sec}) \tag{3.6b}$$

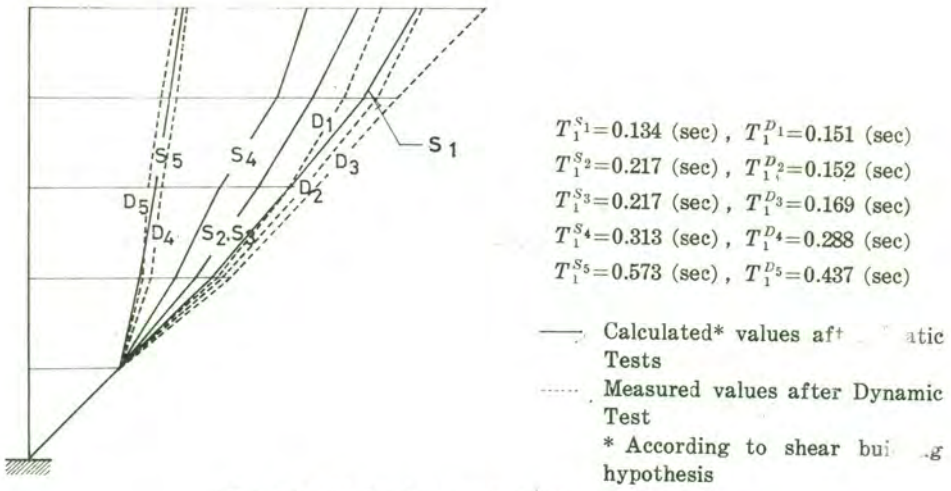

Fig. 3.2. Mode shapes of the 5-story building

In Fig. 3.2. a graphical presentation of the above results is tried. For the sake of clarity the mode shapes are depicted not as appear in the above eigen vectors i,e. unit displacements at level 5, but after some normalization to unit displacements at level 1.

3b. Dynamic tests

The dynamic equation of the free undamped oscillation in matrix form:

$$[K]\{\delta\}_i = \omega_i^2[M]\{\delta\}_i\ , \tag{3.7}$$

was used again, where the matrix $[M]$ as an inherent property of the system is known.

After every dynamic test ω_i^2 and the corresponding mode shape

$\{\delta\}_i$ were determined.

Expanding on the right hand side term of eq. 3.7. gives:

$$\omega_i^2[M]\{\delta\}_i=\omega_i^2\begin{bmatrix} m_1 & 0 & 0 & 0 & 0 \\ 0 & m_2 & 0 & 0 & 0 \\ 0 & 0 & m_3 & 0 & 0 \\ 0 & 0 & 0 & m_4 & 0 \\ 0 & 0 & 0 & 0 & m_5 \end{bmatrix}\begin{Bmatrix} \delta_{1i} \\ \delta_{2i} \\ \delta_{3i} \\ \delta_{4i} \\ \delta_{5i} \end{Bmatrix}=\begin{Bmatrix} \omega_i^2 m_1\delta_{1i} \\ \omega_i^2 m_2\delta_{2i} \\ \omega_i^2 m_3\delta_{3i} \\ \omega_i^2 m_4\delta_{4i} \\ \omega_i^2 m_5\delta_{5i} \end{Bmatrix} \tag{3.8a}$$

though the left hand side term of eq. 3.7 gives:

$$[K]\{\delta\}_i=\begin{Bmatrix} K_{11}\delta_{1i}+K_{12}\delta_{2i} \\ K_{21}\delta_{1i}+K_{22}\delta_{2i}+K_{23}\delta_{3i} \\ K_{32}\delta_{2i}+K_{33}\delta_{3i}+K_{34}\delta_{4i} \\ K_{43}\delta_{3i}+K_{44}\delta_{4i}+K_{45}\delta_{5i} \\ K_{54}\delta_{4i}+K_{55}\delta_{5i} \end{Bmatrix} \tag{3.8b}$$

For shear buildings yields also after [1]:

$$\left.\begin{aligned} K_{ii}&=K_i+K_{i+1}\,, \\ K_{i,i-1}&=-K_i\,, \\ K_{i,i+1}&=-K_{i+1}\,, \end{aligned}\right\} \tag{3.9}$$

which leads to the final equation:

$$[K]\{\delta\}_i=\begin{Bmatrix} K_1\delta_{1i}-K_2(\delta_{2i}-\delta_{1i}) \\ K_2(\delta_{2i}-\delta_{1i})-K_3(\delta_{3i}-\delta_{2i}) \\ K_3(\delta_{3i}-\delta_{2i})-K_4(\delta_{4i}-\delta_{3i}) \\ K_4(\delta_{4i}-\delta_{3i})-K_5(\delta_{5i}-\delta_{4i}) \\ K_5(\delta_{5i}-\delta_{4i}) \end{Bmatrix}=\begin{Bmatrix} \omega_i^2 m_1\delta_{1i} \\ \omega_i^2 m_2\delta_{2i} \\ \omega_i^2 m_3\delta_{3i} \\ \omega_i^2 m_4\delta_{4i} \\ \omega_i^2 m_5\delta_{5i} \end{Bmatrix} \tag{3.10}$$

From this equation the following is easily obtained:

$$\left.\begin{aligned} \frac{1}{f_1}=K_1&=\frac{\omega_i^2}{\delta_{1i}}\sum_{r=1}^{5} m_r\delta_{ri}\,, \\ \frac{1}{f_1}=K_2&=\frac{\omega_i^2}{\delta_{2i}-\delta_{1i}}\sum_{r=2}^{5} m_r\delta_{ri}\,, \\ &\cdots\cdots\cdots\cdots\cdots\cdots\cdots \\ \frac{1}{f_5}=K_5&=\frac{\omega_i^2}{\delta_{5i}-\delta_{4i}}m_5\delta_{5i}\,, \end{aligned}\right\} \tag{3.11}$$

The storey flexibility indices were further normalized to the same natural undamped frequency as for the static tests. This was done in order to have comparable results.

Miscellaneous phenomena, like dissipation of energy through the foundation and the neighboring half space, highly affected the resultant frequencies of the dynamic tests, according to the law $\omega_d=\omega_i\sqrt{1-\zeta^2}$, were ω_d is this resultant (damped) frequency.

3b1. Dynamic Test D_1

Substitution in eqs. 3.11 by the arithmetic values of δ_{ri} (eq. 3.4a), received from the present dynamic test, and $\omega_1^{S_1}=46.95\,(\text{sec}^{-1})$ leads to the calculation of the indices f_r. The final expression of the corresponding flexibility matrix gives:

$$[F]^{D_1}=10^{-6}\begin{Vmatrix} 5.700 & 5.700 & 5.700 & 5.700 & 5.700 \\ 5.700 & 12.393 & 12.393 & 12.393 & 12.393 \\ 5.700 & 12.393 & 18.274 & 18.274 & 18.274 \\ 5.700 & 12.393 & 18.274 & 24.816 & 24.816 \\ 5.700 & 12.393 & 18.274 & 24.816 & 35.300 \end{Vmatrix} (mt^{-1}) \quad (3.12)$$

3b2. Dynamic Test D_2

Following the above described procedure for δ_{ri} received from the present dynamic test and normalization to $\omega_1^{S_2}=28.921\,(\text{sec}^{-1})$, we get:

$$[F]^{D_2}=10^{-6}\begin{Vmatrix} 13.940 & 13.940 & 13.940 & 13.940 & 13.940 \\ 13.940 & 31.382 & 31.382 & 31.382 & 31.382 \\ 13.940 & 31.382 & 47.169 & 47.169 & 47.169 \\ 13.940 & 31.382 & 47.169 & 68.208 & 68.208 \\ 13.940 & 31.382 & 47.169 & 68.208 & 97.143 \end{Vmatrix} (mt^{-1}) \quad (3.13)$$

3b3. Dynamic Test D_3

The same procedure as described above for δ_{ri} after the dynamic test and normalization to $\omega_1^{S_3}=28.921\,(\text{sec}^{-1})$, yields to:

$$[F]^{D_3}=10^{-6}\begin{Vmatrix} 13.039 & 13.039 & 13.039 & 13.039 & 13.039 \\ 13.039 & 30.179 & 30.179 & 30.179 & 30.179 \\ 13.039 & 30.179 & 45.363 & 45.363 & 45.363 \\ 13.179 & 30.179 & 45.363 & 67.388 & 67.388 \\ 13.039 & 30.179 & 45.363 & 67.388 & 116.798 \end{Vmatrix} (mt^{-1})$$

3b4. Dynamic Test D_4

The corresponding values of δ_{ri} are taken from the results of the dynamic test and the $\omega_1^{S_4}=20.096\,(\text{sec}^{-1})$. Thus giving:

$$[F]^{D_4}=10^{-6}\begin{Bmatrix} 56.477 & 56.477 & 56.477 & 56.477 & 56.477 \\ 56.477 & 79.409 & 79.409 & 79.409 & 79.409 \\ 56.477 & 79.409 & 89.876 & 89.876 & 89.876 \\ 56.477 & 79.409 & 89.876 & 110.496 & 110.496 \\ 56.477 & 79.409 & 89.876 & 110.496 & 142.172 \end{Bmatrix} (mt^{-1})$$

3b5. Dynamic Test D_5

The values of δ_{ri} are from eq. 3.5a and freqeuncy to which the values have been normalized $\omega_1^{S_5}=10.949\,(\text{sec}^{-1})$. Then:

$$[F]^{D_5}=10^{-6}\begin{Bmatrix} 204.959 & 204.959 & 204.959 & 204.959 & 204.959 \\ 204.959 & 264.141 & 264.141 & 264.141 & 264.141 \\ 204.959 & 264.141 & 290.297 & 290.297 & 290.297 \\ 204.959 & 264.141 & 290.297 & 360.499 & 360.499 \\ 204.959 & 264.141 & 290.297 & 360.499 & 521.074 \end{Bmatrix} (mt^{-1})$$

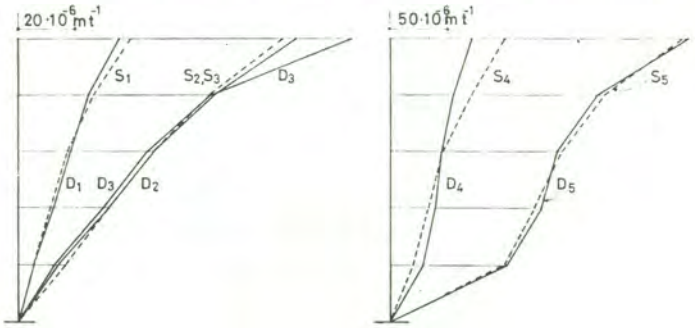

$T_1^{S_1}=0.134$ (sec), $T_1^{S_2S_3}=0.217$ (sec), $T_1^{S_4}=0.313$ (sec), $T_1^{S_5}=0.573$ (sec).

Fig. 3.3. Flexibility coefficients f_{ii}.

In Fig. 3.3 a graphical presentation of the diagonal elements f_{ii} of the flexibility matrices after dynamic and static tests is given.

Part II. Behaviour of the 5-storey Building against Dynamic Loads.

In the present study is assumed as dynamic loads earthquake mo-

tions acting at the foundation of the building. In the whole study the following general assumptions are maintained:

a) The masses of the structure are concentrated respectively at the 5 floor levels.

b) All relative concerning shear buildings.

c) Interstory viscous damping or internal viscous damping. This kind of damping is proportional to the relative velocity between two adjacent floor levels.

d) The horizontal ground motion $y(t)$ is parallel to the long axis of the building, i.e. the axis to which refers the experiment which took place.

e) The structure is symmetrical with respect to the abovementioned axis in item *d*.

This study was performed by means the A. C. type Hitachi model ALM 502T installed at IISEE, and the D. C. type Toshiba model TOSBAC 3400 installed at the same institute.

4. Linear Response Analysis of the Structure Fixed at Base.

The Acceleration $\ddot{y}(t)$ of the sinusoidal function $y(t)=a\sin(\omega_0 t)$ is assumed to be the excitation of the structure. The period of the ground vibration is changed from $T_0=0.02$ sec to $T_0=1.5$ sec with a changeable step of $T_0=0.1000$ sec and $T_0=0.0001$ sec in the resonance regions, in order to draw the resonance curves. The use of suitable time scaling gave the possibility to extend the study with satisfactory accuracy even beyond the 5-th normal mode of the structure, using the abovenentioned A. C. Using a considerable small half amplitude "a", the normal modes were calculated from the solutions by A. C. and satisactorily compared to those obtained after D. C.

a. Study of the Uncracked Structure.

After S_1 were received the coefficients f_{ij}, simplified according to hear building hypothesis. The storey flexibility indices and the corresponding storey stiffness indices are:

$$f_1=f_{11}=5.490\times10^{-6}(mt^{-1}) \qquad K_1=\frac{1}{f_1}=182.15\times10^3(tm^{-1})$$

$$f_2=f_{22}-f_{11}=6.309\times10^{-6}(mt^{-1}) \qquad K_2=\frac{1}{f_2}=158.50\times10^3(tm^{-1})$$

$$f_3=f_{33}-f_{22}=5.732\times10^{-6}(mt^{-1}) \qquad K_3=\frac{1}{f_3}=174.55\times10^3(tm^{-1})$$

$$f_4 = f_{44} - f_{33} = 8.535 \times 10^{-6} (mt^{-1}) \qquad K_4 = \frac{1}{f_4} = 117.16 \times 10^3 (tm^{-1})$$

$$f_5 = f_{55} - f_{44} = 13.378 \times 10^{-6} (mt^{-1}) \qquad K_5 = \frac{1}{f_5} = 74.75 \times 10^3 (tm^{-1})$$

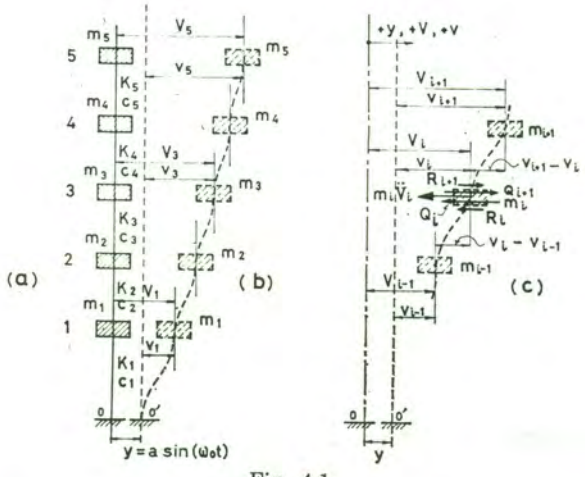

Fig. 4.1.

The dynamic equation for the mass m_i is:

$$-m_i \ddot{V}_i - Q_i + Q_{i+1} - R_i + R_{i+1} = 0 \,, \tag{4.1}$$

where

$$V_i = v_i + y \,, \tag{4.2a}$$

or

$$\ddot{V}_i = \ddot{v}_i + \ddot{y} \,. \tag{4.2b}$$

The force due to internal damping:

$$R_i = C_i(\dot{v}_i - \dot{v}_{i-1}) \,, \tag{4.3}$$

the shear force is:

$$Q_i = K_i(v_i - v_{i-1}) \,, \tag{4.4}$$

where K_i is the storey stiffness index [1].
Eq. 4.1. becomes:

$$-(v_i - v_{i-1})K_i + (v_{i+1} - v_i)K_{i+1} - C_i(\dot{v}_i - \dot{v}_{i-1}) + C_{i+1}(\dot{v}_{i+1} - \dot{v}_i) = m_i \ddot{v}_i + m_i \ddot{y} \,, \tag{4.5a}$$

or:

$$-(v_i-v_{i-1})\frac{m_i}{K_i}+(v_{i+1}-v_i)\frac{K_{i+1}}{m_i}-(\dot{v}_i-\dot{v}_{i-1})\frac{C_i}{m_i}$$

$$+(\dot{v}_{i+1}-\dot{v}_1)\frac{C_{i+1}}{m_i}=\ddot{v}_i+\ddot{y}\ . \tag{4.5b}$$

After dynamic test D_1 the value of $\zeta=2.24\%$.
From the general equation:

$$C=2\zeta\omega_n m\ , \tag{4.6a}$$

Approximately can be used also for the interstorey damping the relation:

$$C_i=2\zeta\omega_n m_i\ . \tag{4.6b}$$

For $\omega_1=46.95\ \text{sec}^{-1}$ (see sect. 3a1) the following table 4.1 is established.

Table 4.1.

i	1	2	3	4	5
$K_i\ (tm^{-1})$	182149.36	158503.72	174459.18	117164.62	74749.58
$m_i\ (tm^{-1}\,\text{sec}^2)$	6.59	6.59	6.59	6.59	4.67
$K_i/m_i\ (\text{sec}^{-2})$	27639.0	24051.0	26473.32	17779.15	16006.33
$K_{i+1}/m_i\ (\text{sec}^{-2})$	24051.0	26473.32	17779.15	11342.88	—
$C_i/m_i\ (\text{sec}^{-1})$	2.1034	2.1034	2.1034	2.1034	2.1034
$C_{i+1}/m_i\ (\text{sec}^{-1})$	2.1034	2.1034	2.1034	1.4905	—

The system of 2nd order differential equations governing the behaviour of the structure, after applying eq. 4.5b, has the form in table 4.2.

A new time variable $\tau=\mu t$ was introduced to faciliate the handling of the problem in the A. C. According to the equations,

$$\tau=\mu t\ , \tag{4.7a}$$

$$\frac{d}{d\tau}=\frac{1}{\mu}\frac{d}{dt}\ ,\qquad \frac{d\tau^2}{d^2}=\frac{1}{\mu^2}\frac{d^2}{dt^2}\ , \tag{4.7b}$$

the system in Table 4.2 is reformed.

A further time scaling was required in order to reduce the fre-

Table 4.2.

$v_1(t)$	$v_2(t)-v_1(t)$	$v_3(t)-v_2(t)$	$v_4(t)-v_3(t)$	$v_5(t)-v_4(t)$	$\dot{v}_1(t)$	$\dot{v}_2(t)-\dot{v}_1(t)$	$\dot{v}_3(t)-\dot{v}_2(t)$	$\dot{v}_4(t)-\dot{v}_3(t)$	$\dot{v}_5(t)-\dot{v}_4(t)$	$\ddot{v}_i(t)+\ddot{y}(t)$
(1)	(2)	(3)	(4)	(5)	(6)	(7)	(8)	(9)	(10)	(11)
−27639.0	+24051.0	—	—	—	−2.1034	+2.1034	—	—	—	$\ddot{v}_1(t)-a\omega_0^2 \sin(\omega_0 t)$
—	−24051.0	+26473.0	—	—	—	−2.1084	+2.1034	—	—	$\ddot{v}_2(t)-a\omega_0^2 \sin(\omega_0 t)$
—	—	−26473.0	+17779.0	—	—	—	−2.1034	+2.1034	—	$\ddot{v}_3(t)-a\omega_0^2 \sin(\omega_0 t)$
—	—	—	−17779.0	+11343.0	—	—	—	−2.1034	+1.4905	$\ddot{v}_4(t)-a\omega_0^2 \sin(\omega_0 t)$
—	—	—	—	−16006.0	—	—	—	—	−2.1034	$\ddot{v}_5(t)-a\omega_0^2 \sin(\omega_0 t)$

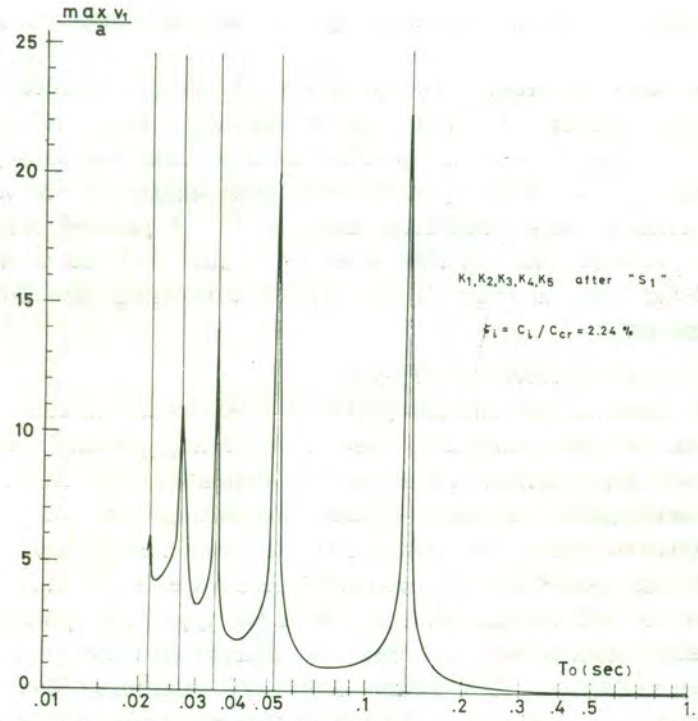

Fig. 4.2. Resonance curve of uncraked structure on rigid foundation-linear behaviour.

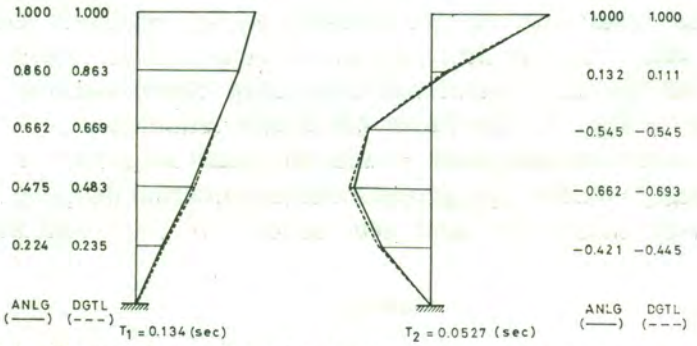

Fig. 4.3. First and second mode shapes of uncracked structure on rigid foundation.

quency error in regions of angular frequencies $\omega_0 > 70.0\,(\text{sec}^{-1})$. In this case the time scaling was set with $\mu = 31.62$. On the other hand an appropriate value of the variable half amplitude "a" was used in order to maintain the amplitute accuracy of the whole problem as high

as possible and to prevent overloadings in the reasonance regions as well.

For the sake of brevity the program of analog computer for the solution of the system of Table 4.2 is abridged here. All solutions $(v_i(t)-v_{i-1}(t))$ of this system are plotted as time functions as long as the excitation occurs. The natural periods and mode shapes of the structure under consideration were calculated after D. C. A perfect coincidence was proved between the results after D. C. and A. C. as is shown in Fig. 4.2 and Fig. 4.3. In Fig. 4.2 the results concerning the first storey only are depicted.

4.b. Study of the Cracked Structure

In some cases of the common practice it is useful enough to know the behaviour of the structure when it is already partially damaged. When a second shock strikes the structure soon after the first one, f.e. Tokachioki-Earthquake, or later on and the damage of the structure is still unrepaired, then, the case under consideration is been realized. The fundamental period of the uncracked structure is $T_1=0.134$ sec. As this structure is stiff enough and of the shear type, its dynamical behaviour against earthquake motions will almost coinside with its first mode of free vibration. This means that the maximum shear forces will be developed at the lower storeys of the structure where also the damage is concentrated. This was proved after the Tokachi-oki and other earthquakes, as well as after the experiment. Especially S_4 and S_5 proved this behaviour. In the present section stiffness coefficients have been taken for the first and second storey those resulting from S_5, though for the third, fourth and fifth storeys those resulting from S_1.

Refering to Fig. 4.1 the Table 4.3 is now established.

The structure showed after D_5 and the small amplitude a final internal damping $\zeta=3.26\%$, though the resultant internal damping between D_1 and D_3 were almost the same (see section *2.b*), it is well known [5]

Table 4.3.

i	1	2	3	4	5
K_i (tm^{-1})	5000.0	18960.0	174459.18	117164.62	74749.58
m_i $(tm^{-1}\,sec^2)$	6.59	6.59	6.59	6.59	4.67
K_i/m_i (sec^{-2})	758.725	2877.09	26473.32	17779.15	16006.33
K_i/m_i (sec^{-2})	2877.07	26473.32	11342.88	11342.88	—

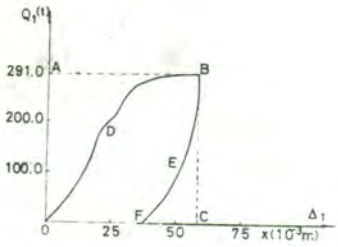

$$Z_1=\frac{(\text{ODBEFO})}{(\text{OABCO})}=\frac{9.55\,tm}{17.0235\,tm}=0.561$$

(a)

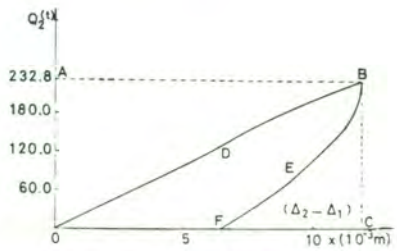

$$Z_2=\frac{(\text{ODBEFO})}{(\text{OABCO})}=\frac{0.952\,tm}{2.770\,tm}=0.344$$

(b)

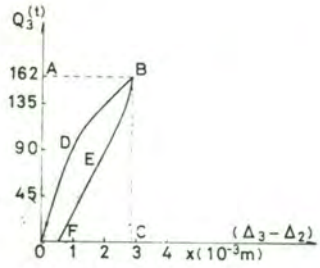

$$Z_3=\frac{(\text{ODBEFO})}{(\text{OABCO})}=\frac{0.1302\,tm}{0.4666\,tm}=0.279$$

(c)

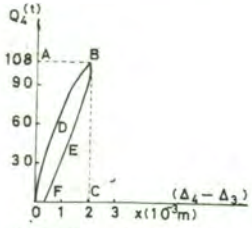

$$Z_4=\frac{(\text{ODBEFO})}{(\text{OABCO})}=\frac{0.2268\,tm}{0.059\,tm}=0.260$$

(d)

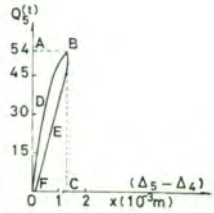

$$Z_5=\frac{(\text{ODBEFO})}{(\text{OABCO})}=\frac{0.0170\,tm}{0.0702\,tm}=0.242$$

(e)

Fig. 4.4a. Load-deflection curve for the first story after S_5.
b. Load-deflection curve for the second story after S_5.
c. Load-deflection curve for the third story after S_3.
d. Load-deflection curve for the fourth story after S_3.
e. Load-deflection curve for the fifth story after S_3.

Table 4.4.

i	1	2	3	4	5
C_i/m_i (sec^{-1})	1.265	0.7745	0.6290	0.5863	0.5458
C_{i+1}/m_i (sec^{-1})	0.7745	0.6290	0.5863	0.3868	—

Table 4.5.

$v_1(t)$	$v_2(t)-v_1(t)$	$v_3(t)-v_2(t)$	$v_4(t)-v_3(t)$	$v_5(t)-v_4(t)$	$\dot{v}_1(t)$	$\dot{v}_2(t)-\dot{v}_1(t)$	$\dot{v}_3(t)-\dot{v}_2(t)$	$\dot{v}_4(t)-\dot{v}_3(t)$	$\dot{v}_5(t)-\dot{v}_4(t)$	$\ddot{v}_i(t)+\ddot{y}(t)$
(1)	(2)	(3)	(4)	(5)	(6)	(7)	(8)	(9)	(10)	(11)
−758.73	−2877.09	—	—	—	−1.265	+0.7745	—	—	—	$\ddot{v}_1(t)-a\omega_0^2 \sin(\omega_0 t)$
—	−2877.09	+26473.32	—	—	—	−0.7745	+0.6290	—	—	$\ddot{v}_2(t)-a\omega_0^2 \sin(\omega_0 t)$
—	—	−26473.32	+17779.15	—	—	—	−0.6290	+0.5863	—	$\ddot{v}_3(t)-a\omega_0^2 \sin(\omega_0 t)$
—	—	—	−17779.15	+11342.88	—	—	—	−0.5863	+0.3868	$\ddot{v}_4(t)-a\omega_0^2 \sin(\omega_0 t)$
—	—	—	—	−16006.33	—	—	—	—	−0.5458	$\ddot{v}_5(t)-a\omega_0^2 \sin(\omega_0 t)$

that damping is proportional to the ratio Z_i between the stored and dissipated energy during cyclic loading statically applied.

The interfloor viscous damping is calculated as follows:

In Fig. 4.4a through 4.4e hysteretic loops (positive part only) are depicted corresponding to the first and second storey for S_5 and to the third, fourth and fifth for S_3 respectively. Also the abovementioned ratios Z_i have been calculated for each storey. If it will be assumed as:

$$\zeta_i = \frac{C_i}{C_{cr}} \frac{5\zeta}{\sum_{i=1}^{5} Z_i} Z_i \,, \tag{4.8a}$$

then

$$\zeta_1 = 5.424\%,\ \zeta_2 = 3.322\%,\ \zeta_3 = 2.698\%,\ \zeta_4 = 2.515\%,\ \zeta_5 = 2.341\%. \tag{4.8b}$$

Using the eq. 4.6b for $\omega_1 = 11.657\ (\text{sec}^{-1})$ the following Table 4.4 is established.

Substitution of the coefficients of Tables 4.4 and 4.3 to the eq.

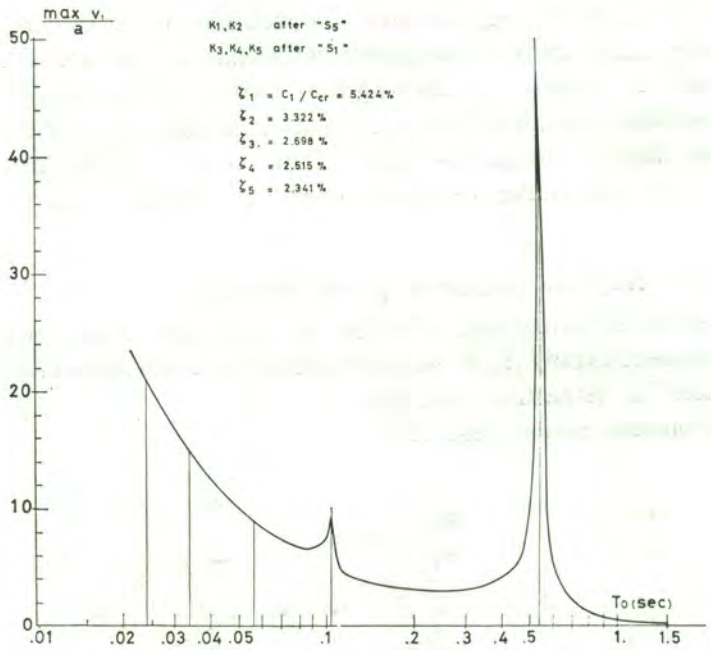

Fig. 4.5. Resonance curve of cracked structure on rigid foundation-linear behaviour.

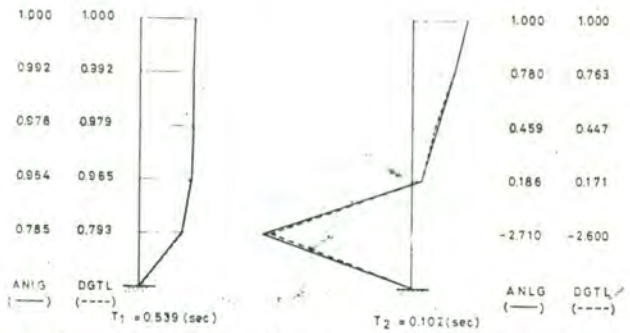

Fig. 4.6. First and second mode shapes of cracked structure on rigid foundation

4.5b the following system in Table 4.5 governing the dynamical behaviour of the system is received. Now systems and the corresponding A. C. circuits (not presented here) with respect to a new time variable $\tau=\mu t$ for $\mu=10$ and $\mu=31.62$ are established. The solutions $v_1(t)/a$ are plotted in Fig. 4.5. In Fig. 4.6 a perfect coincidence for the first and second modes between the solutions received after A. C. and D. C. is shown. As is shown in Fig. 4.6 and the solution by A. C. the upper storeys are very little stressed compared with that of uncracked model.

In Fig. 4.5 no peaks for the higher modes are presented. The first storey oscillates in almost constant period though the upper storeys undergo some higher frequencies and show more evident resonance phenomena. The first storey resonance curve is similar to that of one mass model.

5. *Non Linear Response Analysis of the Structure*

For the sake of comparison of what is done and what might be done in the present study it is roughly refered to some simplified forms of nonlinearities in structures such as:

a. Elastoplastic model (Fig. 5.1)

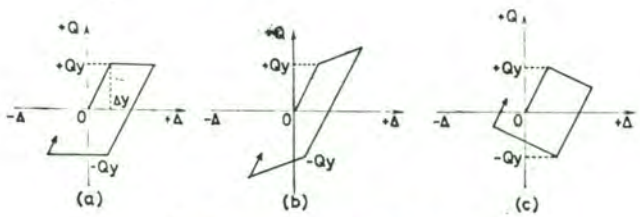

Fig. 5.1. Elastoplastic model.

b. Trilinear model (Fig. 5.2)

Fig. 5.2. Trilinear model.

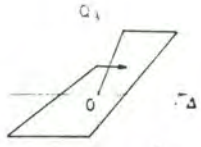

Fig. 5.3. Shear failure model.

c. Shear failure model (Fig. 5.3)

Both stiffness and strength decrease for every yielding. This type of hysteresis property will be suitable for the structure whose damage is caused by the shearing failure of columns.

Studying nonlinearities, care must be paid to the fact that the structure is changing properties within, and in some cases, out of the time interval of the excitation. That means that the damping factor as well as the whole system of differential equations governing the behaviour of the structure must be checked up for every part of the nonlinear form. In the present study it is assumed that nonlinear phenomena can only occur in the columns. In this case the shear type behaviour of the building is coming to be more and more obvious, as more and more columns undergo plastic deformation.

5a. Study of the Nonlinear Elastoplastic Form (I)

The general equation of motion of the i^{th} mass of the idealized system in Fig. 4.1 recalling eq. 4.5b:

$$-(v_i-v_{i-1})\frac{K_i}{m_i}+(v_{i+1}-v_i)\frac{K_{i+1}}{m_i}-(\dot{v}_i-\dot{v}_{i-1})\frac{C_i}{m_i}+(\dot{v}_{i+1}-\dot{v}_i)\frac{C_{i+1}}{m_i}=\ddot{v}_i+\ddot{y}\ , \tag{4.5b}$$

Substitution of eq. 4.4 to eq. 4.5b, leads to:

$$-\frac{Q_i}{m_i}+\frac{Q_{i+1}}{m_i}-\frac{C_i}{m_i}(\dot{v}_i-\dot{v}_{i-1})+\frac{C_{i+1}}{m_i}(\dot{v}_{i+1}-\dot{v}_i)=\ddot{v}_i+\ddot{y}\ , \tag{5.1}$$

The values of K_i, C_i in eq. 4.5b were taken from the results of S_3 and D_3 respectively, i.e.:

$$K_1=1/f_1=6.000\times10^4(tm^{-1})\ , \tag{5.1a}$$

$$K_2=1/f_2=6.646\times10^4(tm^{-1})\ , \tag{5.1b}$$

$$K_3=1/f_3=6.353\times10^4(tm^{-1})\ , \tag{5.1c}$$

$$K_4=1/f_4=5.143\times10^4(tm^{-1})\ , \tag{5.1d}$$

$$K_5 = 1/f_5 = 3.857 \times 10^4 (tm^{-1}) \,, \tag{5.1e}$$

$$C_i/m_i = C_2/m_1 = C_3/m_2 = C_4/m_3 = 2.1034 \,(\sec^{-1}) \,,\quad C_5/m_4 = 1.4905 \,(\sec^{-1}) \,. \tag{5.2}$$

The yielding strength of all 5 stories is assumed to be the same with that of the first storey, which after S_4 proved $Q_y = 371.25^t$, (Ref. to Fig. 5.4). The corresponding Δ_{iy} will be then:

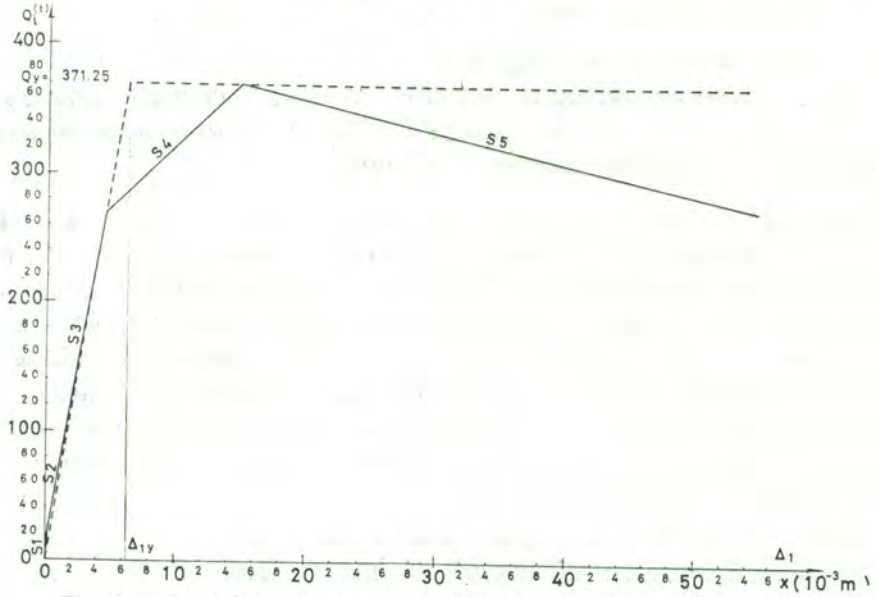

Fig. 5.4. Load-deflection curve for the first storey (average + & −).

$$\Delta_{1y} = Q_y/K_1 = 6.187 \times 10^{-3} (m) \,, \tag{5.3a}$$

$$\Delta_{2y} = Q_y/K_2 = 5.586 \times 10^{-3} (m) \,, \tag{5.3b}$$

$$\Delta_{3y} = Q_y/K_3 = 5.844 \times 10^{-3} (m) \,, \tag{5.3c}$$

$$\Delta_{4y} = Q_y/K_4 = 7.218 \times 10^{-3} (m) \,, \tag{5.3d}$$

$$\Delta_{5y} = Q_y/K_5 = 9.625 \times 10^{-3} (m) \,, \tag{5.3e}$$

During an earthquake excitation the structure starts moving with initial translation and velocity equal to zero. Until the particular differences of the displacements $(v_i(t) - v_{i-1}(t))$ between the adjacent storeys reach the values of Δ_{iy} the phenomenon is absolutely linear. Since some $(v_i(t) - v_{i-1}(t))$ exceed the corresponding value of Δ_{iy} the phenomenon starts its nonlinear behaviour. The value of the particular $+\Delta_{iy}$ is called the upper linear limit though the value of $-\Delta_{iy}$ is called the

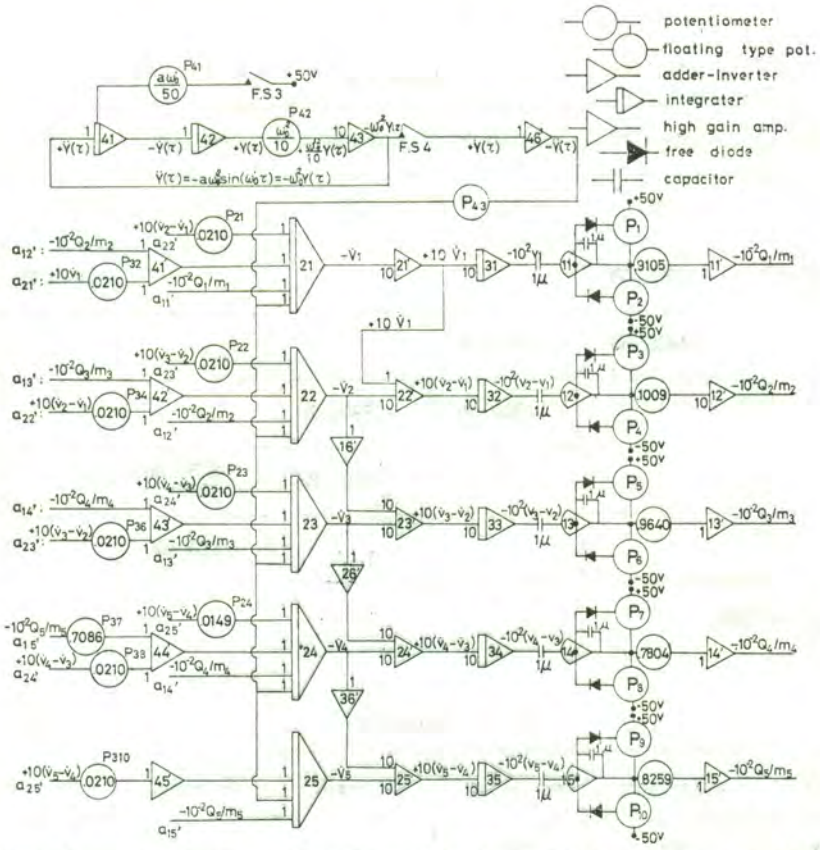

Fig. 5.5. Analog computer program for elasto-plastic behaviour of the structure fixed at base.

lower linear limit. In the present study the absolute values of these two limits are supposed to be the same ar : equal to the corresponding values of eq. 5.3a though e.

In Table 5.1 the system of differential equations governing the behaviour of the system is established, according to eq. 5.1a through e, 5.2 and 5.3a through e. This system in order to be solved by A. C. must be scaled to a new time $\tau = 10t$. The system in the new time reference is shown in table 5.2. On Fig. 5.5 the program for the solution of the system in table 5.2 is presented after [6] and [8].

The first circuit is for the production of the sinusoidal excitation function $\ddot{y}(\tau) = a\omega_0'^2 \sin(\omega_0'\tau)$. As the problem now is not linear the ratios: $\max(v_i(t) - v_{i-1}(t))/a$ are not any more useful, but the absolute values of

Table 5.1.

$v_1(t)$	$v_2(t)-v_1(t)$	$v_3(t)-v_2(t)$	$v_4(t)-v_3(t)$	$v_5(t)-v_4(t)$	$\dot{v}_1(t)$	$\dot{v}_2(t)-\dot{v}_1(t)$
(1)	(2)	(3)	(4)	(5)	(6)	(7)
−9104.70	+10085.00				−2.1034	+2.1034
	−10085.00	+9640.36				−2.1034
		−9640.36	+7804.25			
			−7804.25	+8259.00× 0.7086*		
				−8259.00		

* $\frac{m_5}{m_4}=0.7086$,

Table 5.2.

$v_1(\tau)$	$v_2(\tau)-v_1(\tau)$	$v_3(\tau)-v_2(\tau)$	$v_4(\tau)-v_3(\tau)$	$v_5(\tau)-v_4(\tau)$	$\dot{v}_1(\tau)$	$\dot{v}_2(\tau)-\dot{v}_1(\tau)$
(1)	(2)	(3)	(4)	(5)	(6)	(7)
-91.047 $=-10^{-2}Q_1/m_1$	$+10^{-2}Q_2/m_2$				−0.2103	+0.2103
	-100.85 $=-10^{-2}Q_2/m_2$	$+10^{-2}Q_3/m_3$				−0.2103
		-96.404 $=-10^{-2}Q_3/m_3$	$+10^{-2}Q_4/m_4$			
			-70.043 $=-10^{-2}Q_4/m_4$	$+10^{-2}Q_5/m_5\times$ 0.7086		
				-82.59 $=-10^{-2}Q_5/m_5$		

$\dot{v}_3(t)-\dot{v}_2(t)$	$\dot{v}_4(t)-\dot{v}_3(t)$	$\dot{v}_5(t)-\dot{v}_4(t)$	$\ddot{v}_i(t)+\ddot{y}(t)$	10^3 Upper Linear Limit	10^3 Lower Linear Limit
(8)	(9)	(10)	(11)	(12)	(13)
			$\ddot{v}_1(t)-a\omega_0^2 \sin(\omega_0 t)$	+6.187	−6.187
+2.1034			$\ddot{v}_2(t)-a\omega_0^2 \sin(\omega_0 t)$	+5.586	−5.586
−2.1034	+2.1034		$\ddot{v}_3(t)-a\omega_0^2 \sin(\omega_0 t)$	+5.844	−5.844
	−2.1034	+1.4905	$\ddot{v}_4(t)-a\omega_0^2 \sin(\omega_0 t)$	+7.218	−7.218
		−2.1034	$\ddot{v}_5(t)-a\omega_0^2 \sin(\omega_0 t)$	+9.625	−9.625

$\dot{v}_3(\tau)-\dot{v}_2(\tau)$	$\dot{v}_4(\tau)-\dot{v}_3(\tau)$	$\dot{v}_5(\tau)-\dot{v}_4(\tau)$	$\ddot{v}_i(\tau)+\ddot{y}(\tau)$	10^3 Upper Linear Limit	10^3 Lower Linear Limit
(8)	(9)	(10)	(11)	(12)	(13)
			$\ddot{v}_1(\tau)-a\omega_0'^2 \sin(\omega_0'\tau)$	+6.187	−6.187
+0.2103			$\ddot{v}_2(\tau)-a\omega_0'^2 \sin(\omega_0'\tau)$	+5.586	−5.586
−0.2103	−0.2103		$\ddot{v}_3(\tau)-a\omega_0'^2 \sin(\omega_0'\tau)$	+5.844	−5.844
	−0.2103	+0.1491	$\ddot{v}_4(\tau)-a\omega_0'^2 \sin(\omega_0'\tau)$	+7.218	−7.218
		−0.2103	$\ddot{v}_5(\tau)-a\omega_0'^2 \sin(\omega_0'\tau)$	+9.625	−9.625

$\max(v_i(t)-v_{i-1}(t))$, with respect to the maximum ground acceleration $\max \ddot{y}(t)=a\omega_0^2$. For this reason two series of solutions are provided. The first serie is for $\max \ddot{y}(t)=200$ gal and the second one, after [7], for

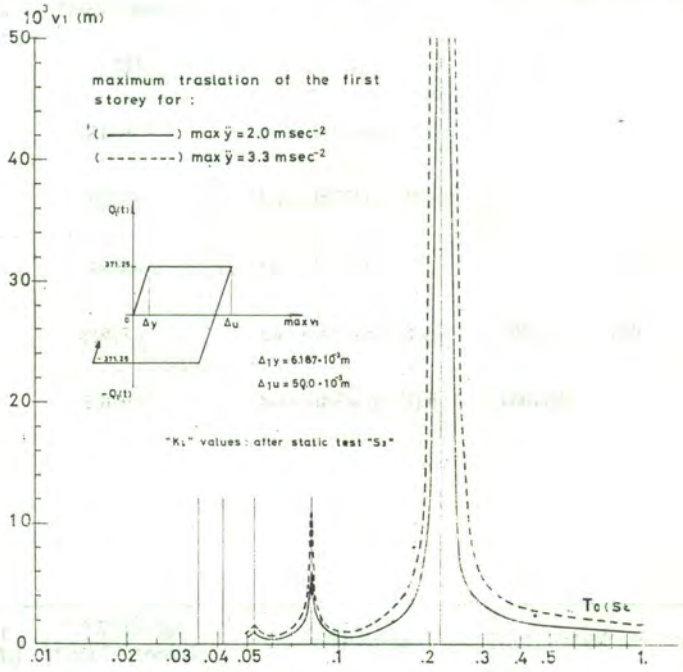

Fig. 5.6. Resonance curves for elasto-plastic behaviour of the structure fixed at base.

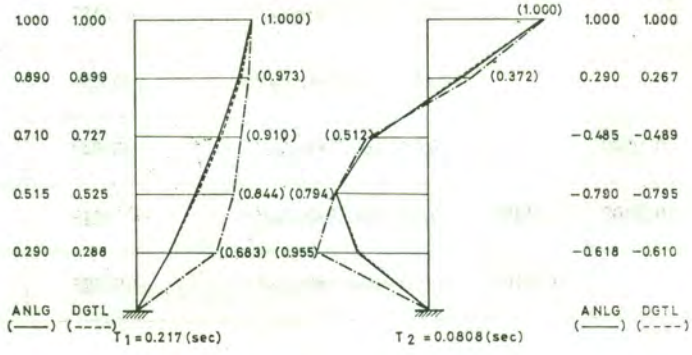

Fig. 5.7. First and second mode shapes for elasto-plastic behaviour of the structure fixed at base.

$\max \ddot{y}(t) = 330$ gal. In Fig. 5.6 the resonance curves for the abovementioned two cases of maximum acceleration are depicted respectively for the first storey. In Fig. 5.7, again a perfect coincidence for the first and second modes between A. C. and D. C., for linear behaviour is shown. The linear solution in A. C. has been achieved by using a considerable small value of maximum acceleration of the exciting function (small value of P_{43} of the program for the exciting function in Fig. 5.5). This actually means use of such $\max \ddot{y}(t)$, so that none of the different storey translations can exceed the corresponding values Δ_{iy} in eq. 5.3a through e. In the same Fig. 5.7 the shapes after yielding according to the A. C. solutions are shown. It is worth while to notice that yielding was occurred at the first and second storeys only. The upper storeys are much less loaded than in the linear case. The effect of the higher acceleration on the upper storeys is not so evident for regions close to resonance, compared to other regions. The shape of the first mode after yielding is similar to that of the cracked structure, as in Fig. 4.6.

5b. Study of the Nonlinear Elastoplastic Form (II)

Besides the structure a nonlinearity is introduced to the yeilding fundations as well, in this part of the paper only problems concerning the superstructure will be discussed. For the remaining part of the design see section 6.

6. Study on the Influence of the Foundation Nonlinear Swinging.

6a. General Assumptions

The vibration system considered in this section is the same as shown in Fig. 6.1, introducing the nonlinearity to both superstructure

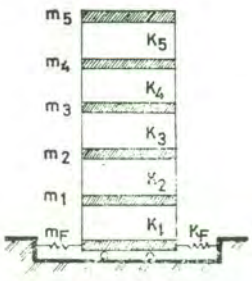

Fig. 6.1. Model of structure.

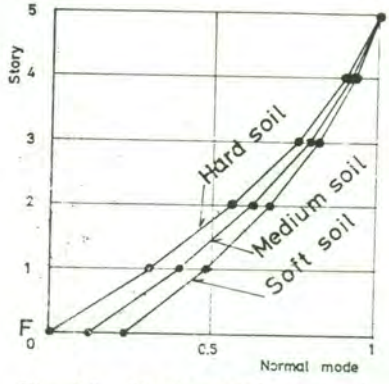

Fig. 6.2. Fundamental normal modes for 3 various soil conditions.

and foundation, in which the effect of the rocking vibration is neglected.

Spring constants of the superstructure are calculated from the slope of the fittest straight line to the hysteresis curve obtained by S_3 test by means of the least square method. Masses at each floor level are determined after consideration of live loads, etc. that are assumed to be located on the actual structure. Spring constants of swinging K_h are given for three various soil conditions. Namely, horizontal soil coefficient C_h is assumed to be ∞, 2 and 1 kg/cm^3 corresponding to hard, medium and soft soils, respectively, from which spring constants K_h are determined. The fixed base conditions are assumed as the case of hard soil.

The fundamental normal modes of those systems are shown in Fig. 6.2, after normalization of the value of the top storey to unity. The damping ratio concerning the fundamental vibration is given as 2.2% equally for all of these systems with the assumption of the internal viscous damping.

6b. Strength and Restoring Force Property

The initial ultimate strength of the superstructure is take as 390 tons uniformly for every storey refering to the result from the static test. Restoring force properties of the structure are presented by the so called shear failure model with the second branch stiffness being zero as shown in Fig. 5.3.

The reduction factors of strength and stiffness are considered to be

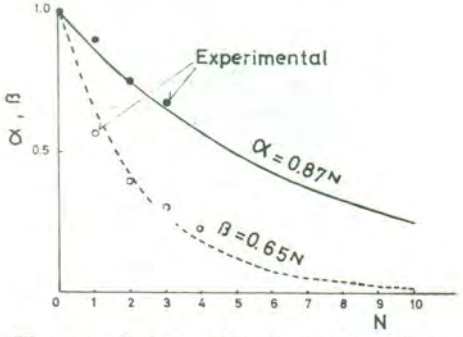

Fig. 6.3. Relation between strength or stiffness reduction factor and yielding number.

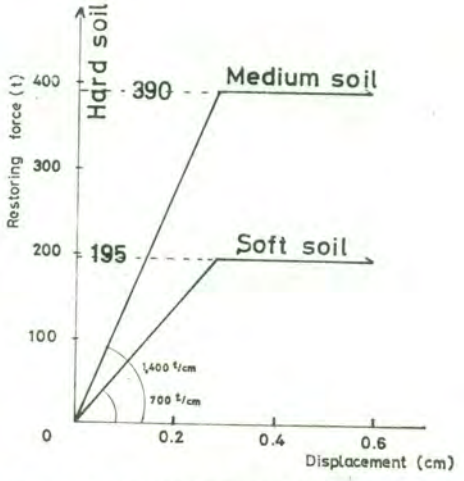

Fig. 6.4. Restoring force characteristics of soils.

the function of number of yielding N and assumed to be expressed by the following equations.

$$\text{The reduction factor of strength } \alpha = a^N \tag{6.1}$$

$$\text{The reduction factor of stiffness } \beta = b^N \tag{6.2}$$

The constants a and b were determined from the experiment as:

$$a = 0.87 \ , \ b = 0.65 \ .$$

The comparison between Eqs. 6.1 or 6.2 and the experimental results are shown in Fig. 6.3.

The strength of soil are assumed to be ∞ for hard soil, 390 tons which is equal to that of the superstructure for medium soil and its half-195 tons for soft soil. The restoring force characteristic of soil is taken as the elasto-plastic type with the second branch stiffness being zero as shown in Fig. 6.4. In this case, the values of α and β are always unity.

Vibration properties obtained from the abovementioned procedure for three various systems are summarized on Table 6.1.

Table 6.1. Vibration properties

Story		Mass ($t \cdot cm^{-1} \cdot sec^2$)	Spring constant ($t \cdot cm^{-1}$)	Ultimate strength (ton)	Yielding displacement (cm)
5		0.0733	423	390	0.922
4		0.0954	589	390	0.661
3		0.0954	636	390	0.614
2		0.0954	616	390	0.635
1		0.0954	564	390	0.690
F	Hard soil	0.239	∞	∞	—
	Medium soil		1450	390	0.279
	Soft soil		700	195	0.279

6c. Ground Motions

Ground motions adopted herein are the band limited white noises which will be considered to be almost equivalent to the actual severe earthquakes [9]. Namely, the ground accelerations $\ddot{y}(t)$ is given by

$$\ddot{y}(t) = 15 \cdot \sum_{n=1}^{100} \cos \{2\pi(10t/n + \varphi_n)\} \ , \ (\text{cm/sec}^2) \tag{6.3}$$

in which φ_n are the random number and $0 \leq \varphi_n \leq 1$.

The duration t_d is taken as 10 seconds. This band limited white noise contains the waves with frequencies 0.1—10 c.p.s. uniformly, and its constant spectral density S_n, the root mean square $\sqrt{\ddot{\bar{y}}^2}$ and the mean maximum acceleration $\ddot{\bar{y}}_{\max}$ are equal to the following values, respectively.

$$S_n = 15 \cdot t_d/2 = 75 \text{ cm/sec} , \tag{6.4}$$

$$\sqrt{\ddot{\bar{y}}^2} = \sqrt{\left(\frac{2}{t_d^2}\right) \cdot \sum_{n=1}^{100} S_n^2} \simeq 106 \text{ cm/sec}^2 , \tag{6.5}$$

$$\ddot{\bar{y}}_{\max} \simeq 335 \text{ cm/sec}^2 . \tag{6.6}$$

Five various band limited white noises with arbitrarily chosen phase angle φ_n were formed and used in the response calculation.

6d. Results of the Response

In Figs. 6.5 and 6.6 shown are the mean maximum absolute acceleration and storey shearing force respectively. The full, dotted and broken lines correspond to the hard, medium and soft soil, respectively.

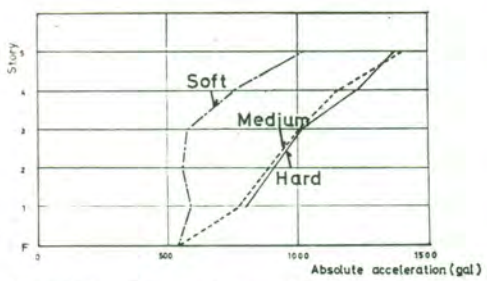

Fig. 6.5. Mean maximum absolute acceleration.

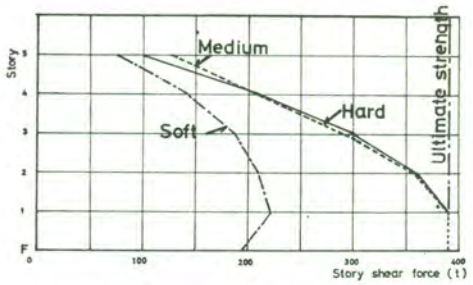

Fig. 6.6. Mean maximum story shear force.

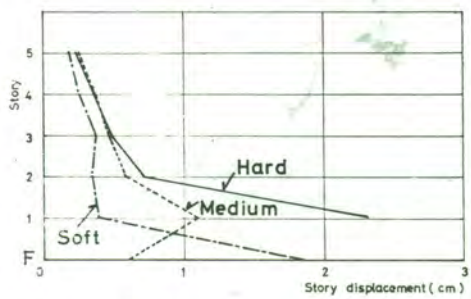

Fig. 6.7. Mean maximum story displacement.

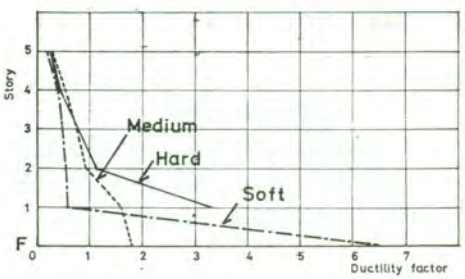

Fig. 6.8. Mean maximum ductility factor.

In case of hard soil, the first storey yields three or four times, but the others do not reach the ultimate strength. In case of medium soil, soil absorbs the vibration energy by yielding two or three times, and number of yielding in the first storey are limited to one or two. In case of soft soil, soil yields as many as 23 or 4 times, and consumes most of energy. Every part in the superstructure remains below the ultimate strength.

In Figs. 6.7 and 6.8 shown are the mean maximum storey displacement and ductility factor, respectively. The abovementioned phenomena will be found more clearly.

Part III. Conclusions & Proposals for Further Research.

It is evident that a generalization of the method evaluating results from dynamic tests can be made.

This can be achieved by determining the frequency matrix $[\omega^2]$ for all the natural periods of the structure. Then instead of the column matrices $\{\delta\}_i$ the shape matrix $[\delta]$ will be obtained. By this way all flexibility coefficients f_{ij} can be determined.

The structure under consideration with wall frames was of the shear type, on account of which the severest damage was concentrated on the lower storeys. If the same structure were much higher than the present one, the damage would be greater in the upper storeys, which means a bending type structure, with shear type frames. The overall behaviour and the resultant concentration of damage in a building with the above modifications will be a subject for further study.

It was proved after the elastoplastic behaviour that once yielding occurred in a part of the structure, then this weakened part undertakes almost the biggest earthquake effect. The rest structure is very little affected from the ground motion. For a 60% bigger ground acceleration, the upper storeys are affected only by 5-10%, in the resonance regions.

In the case of cracked structure—linear behaviour, i.e. very flexible first and second storeys the effect of higher modes was too much reduced, for the lower storeys. The upper storeys were very little loaded, for a ground motion even in the resonance region.

The results obtained from the inelastic response analysis with consideration of the ground effect are summarized as follows.

1) If the ground is considerably hard, this structure will suffer

almost the same damage as that of the final stage of the static test S_5 during the severe earthquake ($\max \ddot{y} = 335$ gal).

2) If the structure stands on the standard soil, the damage by the severe earthquake will be almost in the same condition as that after the static test S_4.

3) If the soil is very soft and has capacity enough to absorb the energy, the damage will remain almost in the same condition as that after the static test S_3.

The authors emphasize the importance of a very flexible construction for the first storey or the first storey-foundation system for structures of the same type with the one considered above. This should be a study for further research.

Acknowledgements

The authors want to express their thanks to Dr. M. Watabe, Chief Research Engineer at IISEE, for his helpfull sugestions to this work.

The graduate students of the Tokyo Electric Engineering College Mr. T. Ohi and Mr. H. Ohura are acknowledged here for their assistance to many calculations herein.

References

[1] KOKINOPOULOS, F. E.: "Approximate Dynamic Aseismic Design of Multistory Systems", *Nat. Tech. Univ. of Athens-Greece.*, **16** (1962).

[2] MERRITT, R. C. & G. W. Housner: "Effect of Foundation Compliance on Earthquake Stresses in Multistory Buildings", *Bull. Seism. Soc. Amer.* **44** (1954), 551-569.

[3] Cherry, S.: "*Dynamics of Structures*" (Lecture Notes No. 5, I. I. S. E. E., 1968).

[4] KOKINOPOULOS, F. E.: "Dynamic Aseismic Design of an Elevated Water Tower", *Bull. Intern. Assoc. for Analog Computation*, **9** (1967).

[5] RUZICKA, J. E.: Editor, "*Structural Damping*", Colloquium on Structural Damping, ASME annual meeting in Atlantic city, N. J. 1959.

[6] FIFER, S.: "*Analogue Computation*", Theory, Techniques and Applications, (McGraw-Hill, 1961).

[7] HOUSNER, G. W.: "Intensity of Earthquake Ground Shaking Near the Causative Fault," *Proc. of the Third World Conference on Earthquake Engineering.*

[8] SERAC Reports, No. 1, 2, 3, 4, 5, 6. c/o *Eng. Res. Inst. Univ. of Tokyo, Japan.*

[9] BYCROFT, G. N.: "White Noise Representation of Earthquakes". *Journal of the ASCE, EM 2*, 1960, 1-16.

Appendix—Photographs

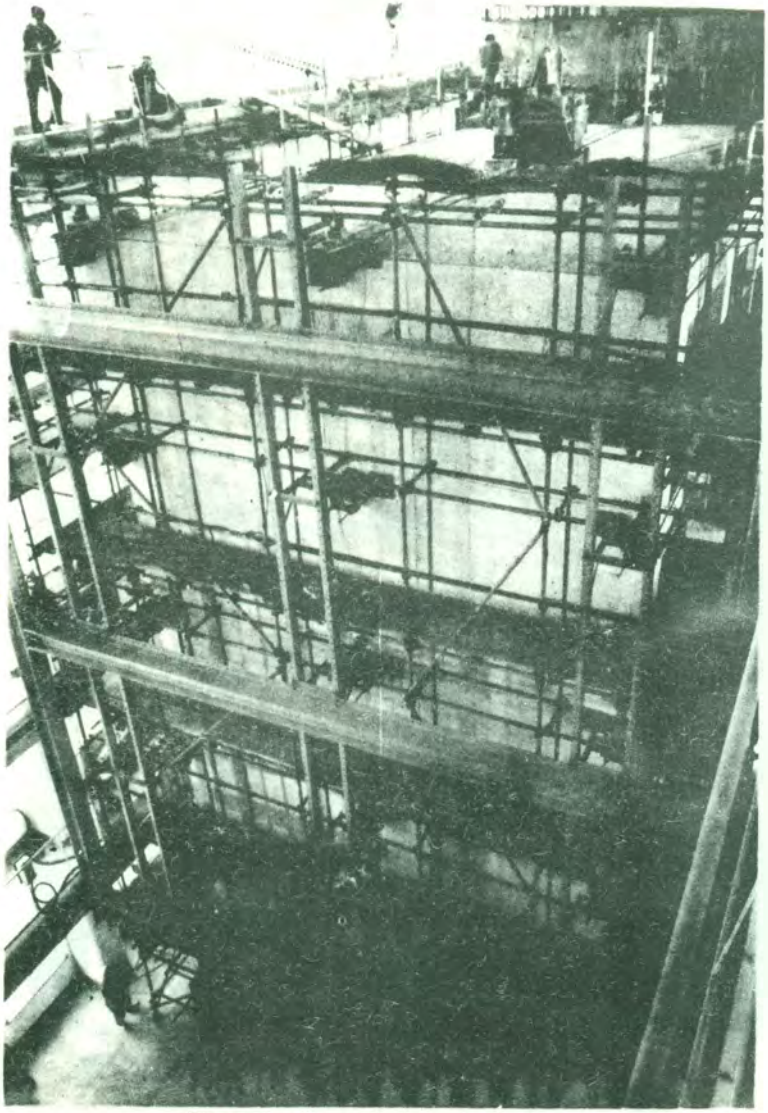

Photo. 1. General view of the test.

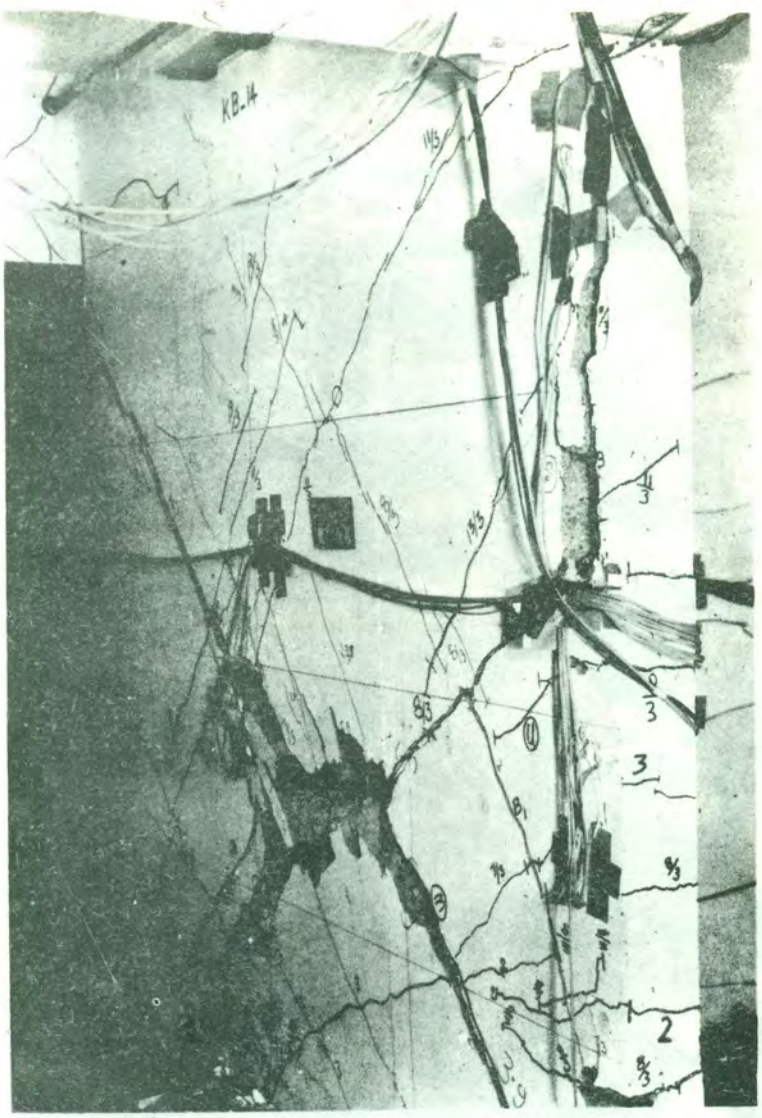

Photo. 2. Failure of the wall column in B-frame (Final stage)